

Illustrating phase transitions with soap films

David R. Lovett and John Tilley

Citation: *Am. J. Phys.* **59**, 415 (1991); doi: 10.1119/1.16520

View online: <http://dx.doi.org/10.1119/1.16520>

View Table of Contents: <http://ajp.aapt.org/resource/1/AJPIAS/v59/i5>

Published by the American Association of Physics Teachers

Additional information on *Am. J. Phys.*

Journal Homepage: <http://ajp.aapt.org/>

Journal Information: http://ajp.aapt.org/about/about_the_journal

Top downloads: http://ajp.aapt.org/most_downloaded

Information for Authors: <http://ajp.dickinson.edu/Contributors/contGenInfo.html>

ADVERTISEMENT



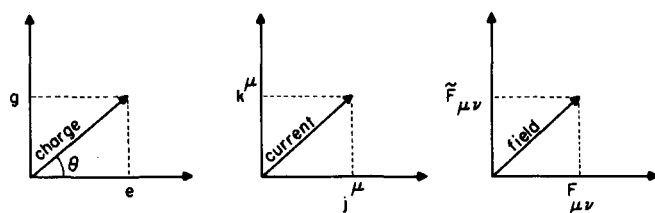


Fig. 1. Two-dimensional charge space.

be written

$$\partial_\nu \begin{pmatrix} F^{\mu\nu} \\ \tilde{F}^{\mu\nu} \end{pmatrix} = -\mu_0 c \begin{pmatrix} j^\mu \\ k^\mu \end{pmatrix}, \quad (19)$$

$$\frac{dp_\mu}{ds} = \frac{1}{mc} \begin{pmatrix} F_{\mu\nu} \\ \tilde{F}_{\mu\nu} \end{pmatrix} p^\nu. \quad (20)$$

Under rotations in charge space, both sides of Eq. (19) transform as vectors, and both sides of Eq. (20) transform as scalars. So our system is invariant under rotations in charge space. An argument that nature favors symmetry would certainly favor this model over conventional electrodynamics.

Now suppose that all charged particles are, in fact, dual-charged particles, and that they all have the same ratio g/e . Then the charge of every particle would have the same angle $\theta = \tan^{-1}(g/e)$ in charge space. Rotating the axes of charge space through the angle θ would then convert

every dual-charged particle to a pure electric monopole, but because of the invariance of the system under this rotation, the behavior of the system would not change. An isolated system of dual-charged particles, all having the same ratio g/e , is therefore indistinguishable from a system of pure electric monopoles. The charge space symmetry, in this case, leads us back to conventional electrodynamics.

V. SUMMARY

The direct development of classical electrodynamics from its symmetries, without recourse to Hamilton's principle, would seem to have some pedagogical advantages. Students can readily determine that Maxwell's equations and the Lorentz force law are the only "simple" dynamical equations having Lorentz covariance and gauge invariance. But these equations presuppose a vector field A^μ . By replacing this vector field by an antisymmetric tensor field $F^{\mu\nu}$, a classical model of magnetic monopoles is immediately developed. Although this latter treatment would not be valid in a quantized model (the vector field A^μ being essential to quantum electrodynamics), it does present, in a simplified way, the classical properties of magnetic monopoles.

¹P. A. M. Dirac, "Quantised singularities in the electromagnetic field," Proc. R. Soc. London Ser. A **133**, 60-72 (1931); "The theory of magnetic poles," Phys. Rev. **74**, 817-830 (1948).

²For an excellent review of the significance of gauge invariance to the theory of particle interactions, see R. Mills, "Gauge fields," Am. J. Phys. **57**, 493-507 (1989).

³J.D. Jackson, *Classical Electrodynamics* (Wiley, New York, 1975), Sec. 11.9.

Illustrating phase transitions with soap films

David R. Lovett and John Tilley

Department of Physics, University of Essex, Colchester CO4 3SQ, United Kingdom

(Received 23 April 1990; accepted for publication 21 August 1990)

First-order and second-order phase transitions are demonstrated using soap-film models. The models consist of two-dimensional parallel plates or three-dimensional frameworks in which film patterns are maintained. By making the sizes of the frameworks variable, it is possible to induce switching between film patterns analogous to transitions between phases. These phase changes are discussed thermodynamically and using a catastrophe theory model.

I. INTRODUCTION

Soap films, set up either between two-dimensional perspex plates that are connected together with pins or within three-dimensional wire frameworks, can be used to demonstrate the phenomenon of minimization of energy¹⁻⁴ and are well known. The effect arises because the surface energy associated with the film is proportional to its area. The tendency for the film to minimize its energy means that it tries to minimize its area. The patterns achieved are both surprising when viewed for the first time and attractive. Analogous patterning can be seen in biological systems and in crystal structures. However, the frameworks used are

usually fixed in size and shape; any sudden change of film pattern that occurs is erratic due to contraction of the film immediately after it has been established and prior to the achievement of equilibrium or is due to external influences such as air currents.

What have received far less attention are frameworks whose size and shape can be varied in a controlled way. Soap-film patterns then switch in a *predictable* manner and the changes are analogous to phase transitions in crystals. Such changes in the soap-film patterns can be quite spectacular to observe. Pattern changes can be quite complex and so the analogy is very illuminating and effective in the teaching of phase transitions. As will be shown in this arti-

cle, mathematical comparisons can be made with both first-order and second-order phase transitions because the underlying thermodynamics is the same. Just as catastrophe theory can be applied to phase transitions, so a catastrophe model can be used for modeling changes in soap-film configurations.

The frameworks can be constructed very easily in a workshop, or it is possible to obtain the patterns using frameworks made with acetate sheets, plastic straws, and matchsticks! Although we refer traditionally to the films as soap films, it is customary to use washing-up liquids or similar detergents.

Although pattern changes as observed in three-dimensional frameworks show the closest analogy to crystal arrangements and biological cell structures that are also three-dimensional, these soap-film configurations are less easy to model mathematically because they involve curved surfaces or curved edges, where the surfaces meet, or both. It is not easy to calculate the curvature of such surfaces. However, soap-film patterns between parallel plates show no such curvatures and are mathematically more tractable. Hence, we will first show phase-transition modeling using films confined between parallel plates.

II. 2-D MODEL; FIRST-ORDER PHASE TRANSITION

In the first example, the film, besides being constrained between the parallel plates, connects four pins as shown in Fig. 1(a). Minimization of area now implies minimization of length and we show the soap-film configuration to join the four points A, B, C, and D. (The shortest length is not a cross.) The continuous and the dashed lines show two alternative and equivalent configurations. Suppose we keep A and B fixed and move pins C and D outward and inward together as shown by the arrows. It is easy to see that the film will switch backward and forward between the two configurations. Provided movement of C and D is done slowly, the film alters such as always to establish the equilibrium shape corresponding to minimum length; see Fig. 1(b). There may be a tendency for some sticking of the film but it will gradually take up the correct shape. If, for instance, one blows the film to move it away from equilibrium, this increases the energy of the film such that there is movement up the energy versus configuration curve. The film then relaxes back to its equilibrium shape.

One can calculate the total length L of the film for any particular separation x by summing the five component lengths together and, by doing this for a range of values of x , can plot a graph of L vs x as shown in Fig. 2(a). There is a portion of the graph with gradient of $\sqrt{3}$ and a portion with gradient 1. The variation of dL/dx with x is shown in Fig. 2(b). The change in gradient occurs as the soap-film pattern changes from its full-line to its dashed-line configuration. Note that the film exhibits hysteresis; the switch happens when the two intersection points of the film meet and this occurs for different values of x during expansion and contraction. The two portions are analogous to the existence of different phases of a material on either side of a transition temperature, and the hysteresis is analogous to superheating and supercooling. What we see is a first-order phase change with a distinct jump in area or volume at the transition.

Thermodynamically, one can consider the Helmholtz free energy, $F = U - TS$, where U is the internal energy, T

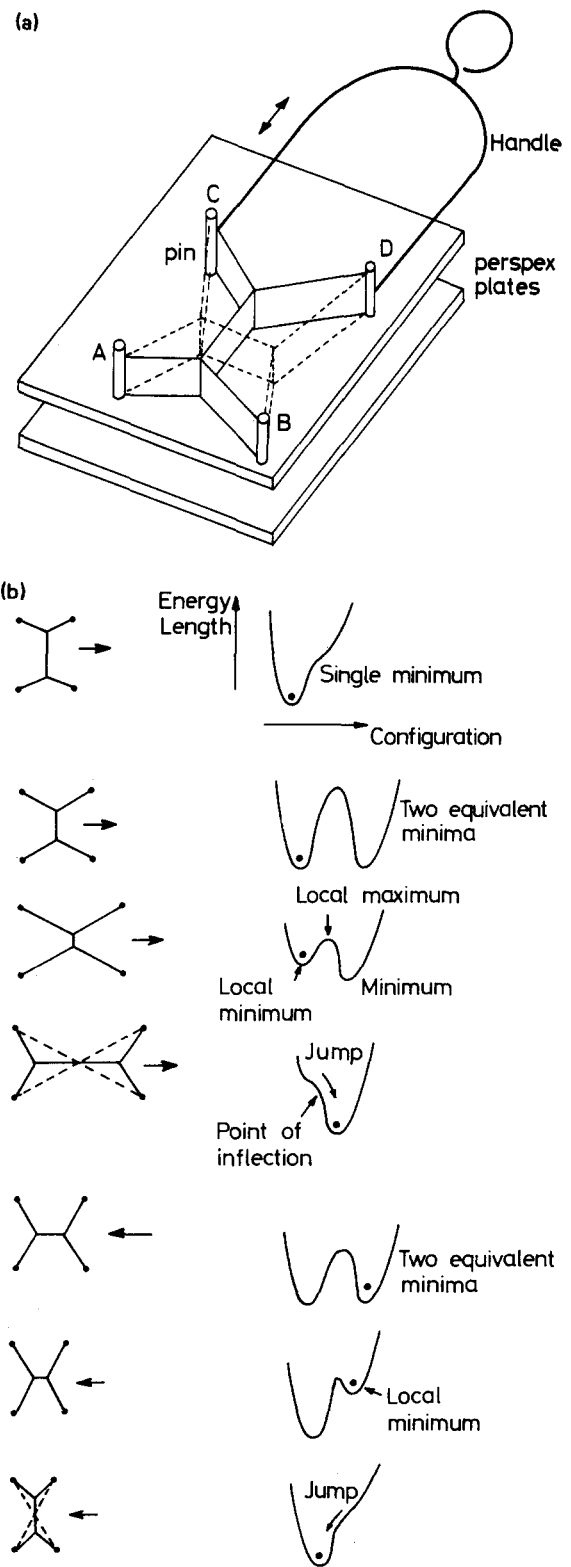


Fig. 1. (a) Film patterns using four pins; (b) Energy versus configuration plots for film patterns corresponding to different separations x of AB and CD.

is Kelvin temperature, and S is entropy. For the Helmholtz function, the independent variables are T and volume V ,^{5,6} so that

$$dF = -S dT - P dV,$$

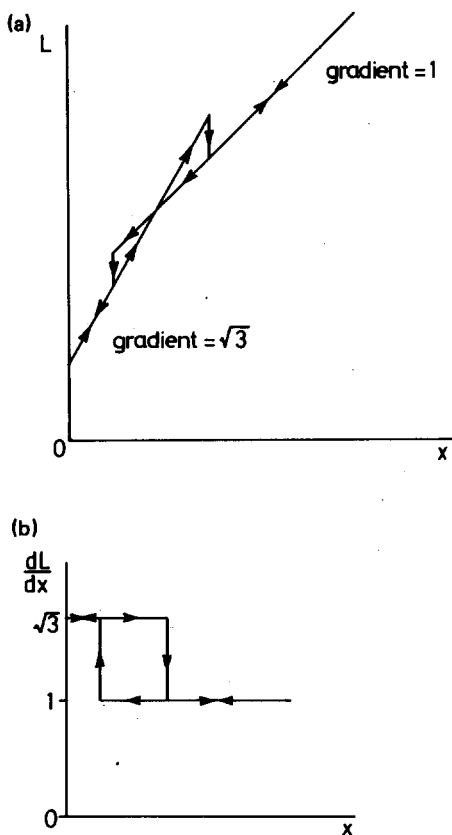


Fig. 2. (a) Variation of soap-film length L with separation x of AB and CD; (b) Variation of dL/dx .

where P is pressure and

$$P = -\left(\frac{\partial F}{\partial V}\right)_T \text{ and } S = -\left(\frac{\partial F}{\partial T}\right)_V.$$

Alternatively, if P and T are the independent variables, we should use the Gibbs free energy $G = U - TS + PV$, in which case

$$dG = -S dT - V dP$$

and

$$V = -\left(\frac{\partial G}{\partial P}\right)_T \text{ and } S = -\left(\frac{\partial G}{\partial T}\right)_P.$$

The gradient dL/dx in Fig. 2 will be equivalent to any of these partial differentials (giving P , V , or S) depending on which analogy one wishes to make. However, the analogy with $P = -(\partial F/\partial V)_T$ is clearly the most appropriate. In fact, the force in the direction of x required to keep pins AB and CD distance x apart is $2T_s h(dL/dx)$, where T_s is the surface tension and h is the height of the pins. This force for the two-dimensional case is analogous to pressure in the three-dimensional case and has the value of $2\sqrt{3}T_s h$ for the low x phase and $2T_s h$ for the high x phase.

III. 2-D MODEL; SECOND-ORDER PHASE TRANSITION

A very different type of transition occurs if we consider only three pins as shown in Fig. 3. Pins A and B are fixed and pin C is variable, moving along the line OCC'. When the movable pin lies within the arc ACB, the film will consist only of two lengths AC and CB. When this pin is out-

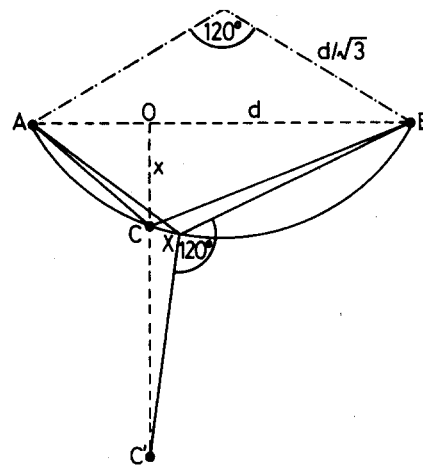


Fig. 3. Film patterns using three pins.

side the arc, the film will consist of lengths AX, XB, and XC with the angles between the lengths all 120° . Again we plot the variation of total film length L with x . The curve now looks smooth as shown in Fig. 4(a) and it is only when we plot the gradient dL/dx vs x , Fig. 4(b), that we obtain a sudden change of gradient characteristic of a phase transition. This occurs at $x = x_0$, where x_0 measures OC, the value of x at the edge of arc ACB. Thus we have a second-order phase transition. It is relatively easy to calculate and plot L vs x and dL/dx vs x but actual plots will depend on the chosen position of O along AB. We can go on to plot d^2L/dx^2 vs x as shown in Fig. 4(c). Now d^2L/dx^2 is equivalent to $(\text{axial compressibility})^{-1}$ or the equivalent thermodynamic quantity as summarized in Table I. Beyond arc ACB, the variation in d^2L/dx^2 arises because the angle $XC'C$ changes and would be zero for O midway between A and B.

A second-order transition involves a lowering of symmetry and we can associate an order parameter with the transition. The highest possible symmetry is that of isotropic bodies whose properties are the same in all directions. In anisotropic bodies the symmetry is lowered. When point C' moves from inside to outside the arc ACB, there is no overall change in the total symmetry of the system. Nevertheless, there is a change of local symmetry about point X. It is appropriate that we categorize the symmetry about this point X as the symmetry at X characterizes the pattern. The lengths of the arms can be of any magnitude without affecting the transition provided the angular relationship is retained.

When C' lies outside the arc ACB there is threefold symmetry about X (i.e., crystallographic symmetry $3m$), whereas when C' lies within the arc there is no particular symmetry (crystallographic symmetry 1). The higher symmetry phase corresponding to when C' lies outside the arc (symmetry $3m$) should correspond to the order parameter having the lower value. Such an order parameter must describe quantitatively the change in structure as it passes through the transition point and must be zero in the symmetrical phase.⁶ An order parameter that gives a variation analogous to that for crystal phase transitions can be defined by

$$Q = (\angle A \times B / 60^\circ - 2)^{1/2}. \quad (1)$$

The power of $\frac{1}{2}$ is in line with phase-transition theory,

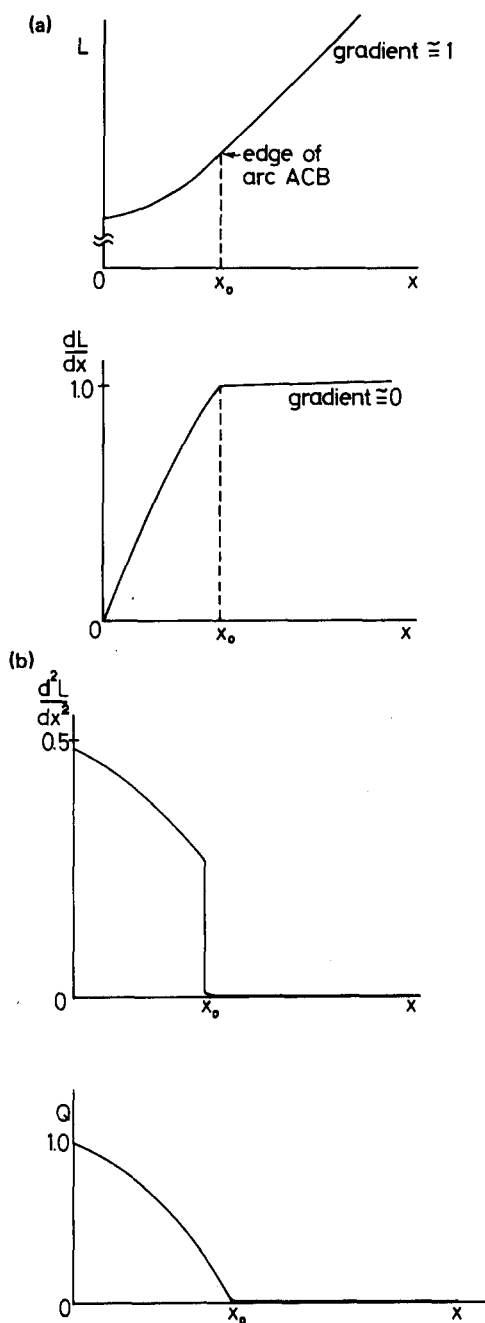


Fig. 4. (a) Variation of soap-film length L with parameter x for three-pin pattern; (b) Variation of dL/dx with x ; (c) Variation of d^2L/dx^2 with x ; (d) Variation of order parameter Q with x .

and it is of similar form to the order parameter that will be found necessary for the next model to be considered. Briefly, the thermodynamic potential Φ for a system involving a phase transition can be expressed in the form

$$\Phi = \Phi_0 + aQ^2 + bQ^4 + \dots, \quad (2)$$

where Φ_0 , a , and b are constants. Φ can be expressed in the soap-film model in the form

$$\Phi = \Phi_0 + a'\alpha + b'\alpha^2 + \dots, \quad (3)$$

where a' and b' are constants and α is an angle. Hence Q is proportional to $\alpha^{1/2}$ and as the constants are undefined we can put $Q = \alpha^{1/2}$.

Note that the structural type of order parameter Q fits with the thermodynamic analogy made with (dG/dP) at constant T . If we were making the analogy with (dG/dT) at constant P , we would need an order parameter in the form of (reduced temperature) $^{1/2}$. However, the surface tension does not change significantly with temperature so this analogy is not possible.

IV. 2-D MODEL; PHASE-TRANSITION AND CATASTROPHE THEORY MODEL

A more general model combines features of the two preceding ones: Not only does it show the first-order phase change when the total film length suddenly contracts, but also the change of symmetry associated with a second-order transition. Such a model can be established using three fixed pins and a fourth pin that is movable. It is more general because it involves two degrees of freedom and as a consequence two order parameters. We could use the arrangement shown in Fig. 1(a). However, a more convenient and symmetrical model is one with the fixed pins at the vertices of an equilateral triangle.⁷ Such a model is shown in Fig. 5. P_0 , P_1 , and P_2 are the fixed pins and C is the movable pin. The two alternative equilibrium film patterns for one position of C are shown, one pattern being shown with full lines and the other with dashed lines. In order to describe the behavior of this model, it is helpful to draw two intersecting circles, one through P_0 , Z , and P_1 , the other through P_0 , Z , and P_2 , where Z is the centroid of the triangle $P_0P_1P_2$. An equilibrium pattern occurs when the film junction lies on one of the circular arcs. If the pattern includes the length CP_2 , the equilibrium junction point J_e lies on the arc P_0ZP_1 because this always subtends an angle $(P_0J_eP_1)$ of 120° . The other two angles at the junction point J_e , P_0J_eC and P_1J_eC , are also 120° , and it is straight-

Table 1. Equivalent thermodynamic quantities.

Thermodynamic function	Helmholtz free energy, F Differential	Experimental quantity	Film energy \propto film length, L Differential	Experimental quantity
First differential	$\left(\frac{\partial F}{\partial V}\right)_T$	pressure, P	$\left(\frac{\partial L}{\partial x}\right)_T$	force
	$\left(\frac{\partial F}{\partial T}\right)_V$	entropy, S		
Second differential	$\left(\frac{\partial P}{\partial V}\right)_T$	1/(isothermal compressibility)	$\left(\frac{\partial^2 L}{\partial x^2}\right)_T$	1/(axial compressibility)
	$\left(\frac{\partial S}{\partial T}\right)_V$	specific heat, C_V		

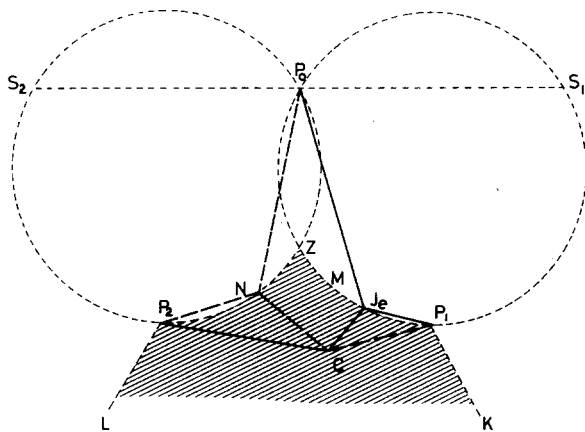


Fig. 5. Film pattern for model involving three fixed pins and a movable pin.

forward to show that J_e lies on the straight line CS_1 . The same argument applies if the pattern includes CP_1 , in which case J_e lies on the arc P_0ZP_2 and on the straight line CS_2 .

One can obtain a mathematical expression for the energy of the model for the general case, whether junction J lies at an equilibrium position or away from such a position. The properties of the model depend on the position and motion of the movable pin C . The following features, which are characteristic of a system displaying catastrophic changes, have been deduced or calculated:

- (1) While C is in the shaded region, two equilibrium patterns are always possible.
- (2) The boundaries of the shaded regions are bifurcation lines separating the plane into certain regions where the model is monostable and others where it is bistable.
- (3) One can show that the length of the film for the configurations shown in Fig. 5 can be expressed as

$$L = AP^2 + BQ^2 + CP^2Q^2 + DP^4 + EQ^4. \quad (4)$$

This is the form of equation used to describe phase diagrams in which there are two order parameters P and Q .⁸ ($A-E$ are constants independent of P and Q .) It is also the form of equation used to describe a double-cusp catastrophe model.⁹

To get the length in the form given by Eq. (2), it is necessary to use two angular parameters to define the position of the junction point J in the plane relative to the control point C . The angles that have been used by the authors are α (angle JS_1C), and β (angle JS_2C). Provided C is not too distant from the cusp point, Z , Eq. (4) is general and applies for J being at nonequilibrium as well as equilibrium positions. The order parameters are given by

$$P = g_\theta(\alpha + \beta)^{1/2} \text{ and } Q = f_\theta(\alpha - \beta)^{1/2}, \quad (5)$$

where g_θ and f_θ involve a theta step function used to define whether P and Q are positive or negative, a requirement arising because the positive square roots are always taken in Eq. (5). The order parameters fit well with that given in Eq. (1) for a single variable model.

Solution of Eq. (4) to obtain the bifurcation lines (the phase boundaries) involves partial differentiation of L with P and Q . The ($P=0, Q=0$) solution gives the high symmetry point at Z . There are also imaginary solutions for P and Q which can be ignored. The important solutions involve coupled equations between P and Q and give arcs

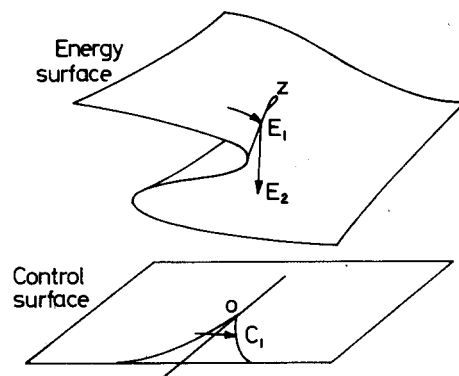


Fig. 6. Cusp catastrophe; energy surface and control plane.

passing through Z and pairs of points P_0, P_1 , and P_2 . Two such arcs are shown in Fig. 5 but there are possible a complete pattern of such arcs, each one passing through two pins. The angle subtended on these arcs by the two pins is always 120° .

The complete model can be represented by a series of cusp catastrophes of the type described by Zeeman.¹¹ A single such cusp catastrophe is shown in Fig. 6. As the control point, i.e., the movable pin, is moved on the control surface, the total energy of the soap film varies according to position on the energy surface. When the control point reaches a bifurcation line, the soap film changes its length and hence its energy. For example, at point C_1 the energy changes from E_1 to E_2 . In the present example, it is as if we had three such surfaces pivoted around the cusp point Z with the surfaces tilted such that they are continuous and hence produce one overall surface. Traveling around the central cusp point Z in a circle in one sense would thus produce three such catastrophic jumps.

V. 3-D MODELS; FIRST-ORDER REVERSIBLE PHASE TRANSITIONS

We now describe models that show changes in soap-film pattern in three dimensions. As stated previously, this has more realistic comparison with transitions in crystalline solids that consist of three-dimensional packing of atoms. Three simple frameworks demonstrate these transitions. Triangular and pentagonal prisms and the cuboid, each with variable height, show distinct transitions between two different configurations. They are illustrated in Fig. 7. In the case of the triangular prism, the soap film switches between a pattern with all curved surfaces and one with flat surfaces. The film always takes on the curved configuration for height less than $0.3 \times$ side length, and always takes on the plane configuration for height equal to side length. Between these values there is hysteresis.

In the case of the cuboid, as its length is increased from a flat shape, there occurs a switch from a square region of film parallel to the square cross section to a rectangular region parallel to a long side. If the cuboidal frame is made carefully, the square region can switch to a rectangular region at right angles in either of two orthogonal planes. This phenomenon can occur during phase transitions in real crystals leading to twinning.

The pentagonal prism exhibits film surfaces that switch from a pattern showing two distinctive vertical planes in the center to a pattern with a horizontal pentagon. Analogous patterns can be formed between parallel perspex

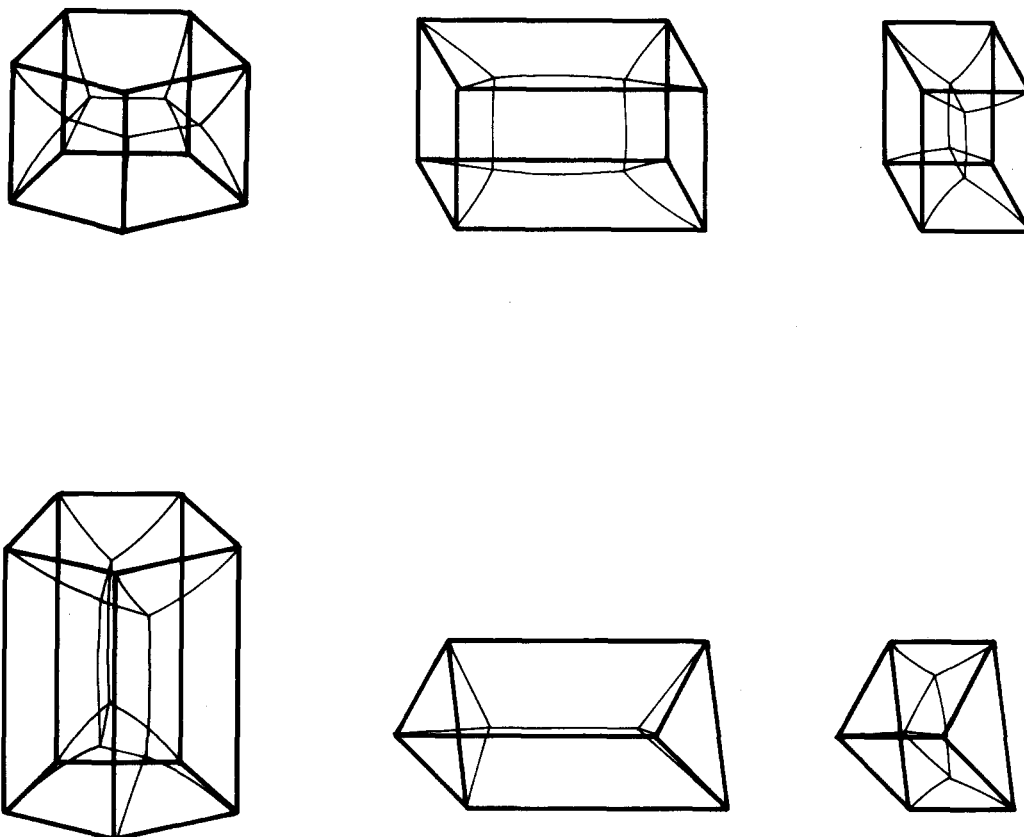


Fig. 7. Soap-film patterns within a triangular prism, a cuboid, and a pentagonal prism.

plates joined by five pins in the configuration of a pentagon, although in this case the central pentagon is a bubble having curved faces. In two dimensions the pentagonal bubble has to be established by suitable dipping of the framework into the soap solution and cannot be obtained by switching.

VI. 3-D MODEL; FIRST-ORDER IRREVERSIBLE PHASE TRANSITION

Another example of a jump between two configurations is a soap film contained within a wedge. The film is held between two pins placed equidistant from the vertex of the wedge. The film bends into the wedge in order to minimize its area (Fig. 8). The bending produces a curve that is a catenary (the shape established by a hanging chain suspended at its ends). Provided the separation of the pins is less than $1.33r$, where r is the perpendicular distance of the pins from the wedge vertex, the film is stable. If the model is

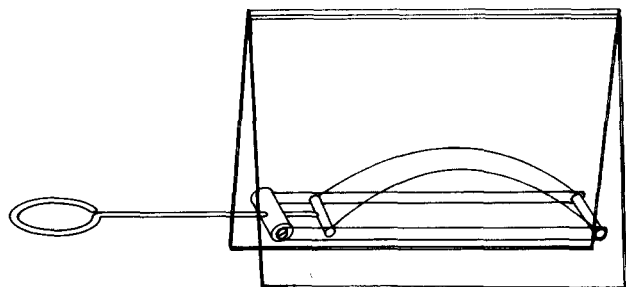


Fig. 8. Film formed within a wedge.

made such that the separation of the pins is variable and is increased to greater than $1.33r$, the film is unstable and slowly moves toward the vertex of the wedge where it splits to form two parallel films. (This is provided the wedge is horizontal and there are no gravity effects. If the wedge is vertical, the gravitational force can stabilize the film, in which case it is possible to see very attractive interference films.) Unlike in the previous models, it is not possible by reversing the motion of the pins to get the film back to its original configuration. The film is a slice of the film set up between two hoops after they have been dipped in solution and opened apart.^{11,3} In the case of separating the two hoops greater than $1.33r$, where r is their radius, the film collapses immediately. The theory of such films has been discussed extensively in the literature.^{12,13} In the case of the wedge, the collapse can be viewed in slow motion.

VII. CONCLUSION

In this paper we have described several different soap-film models that demonstrate various features of first- and second-order phase transitions. However, it is not necessary for students to have a knowledge of phase transitions to appreciate the simple demonstrations of changes of shape occurring as the consequence of the need to minimize energy. The models help in understanding the reasons for differing crystal symmetries and patterns in nature.

¹C. Isenberg, "Problem-solving with soap films," *Phys. Educ.* **10**, 452-456, 500-503 (1975).

²D. R. Lovett, "Soap films, phase changes and catastrophes," *Phys. Educ.* **14**, 40-44 (1979).

³C. Isenberg, *The Science of Soap Films and Soap Bubbles* (Tieto, Cleve-
don, England, 1978).
⁴D. R. Lovett and S. R. P. Smith, "Phase transitions and soap films," *Sch.
Sci. Rev.* **62**, 287–298 (1980).
⁵C. J. Adkins, *Equilibrium Thermodynamics* (McGraw-Hill, London,
1968).
⁶L. D. Landau and E. M. Lifshitz, *Statistical Physics* (Pergamon, Oxford,
1980), Pt. 1, pp. 446–455.
⁷D. R. Lovett and J. Tilley, "A soap film model illustrating phase transi-
tions," *Eur. J. Phys.* **11**, 208–214 (1990).
⁸J-C Tolédano and P. Tolédano, *The Landau Theory of Phase Transitions*

(World Scientific, Singapore, 1987), p. 195.
⁹T. Poston and I. Stewart, *Catastrophe Theory and Its Applications* (Pit-
man, London, 1978), pp. 314–317.
¹⁰E. C. Zeeman, "Catastrophe theory," *Sci. Am.* **234**(4), 65–83 (1976).
¹¹D. R. Lovett and S. R. P. Smith, "Soap films in a wedge," *Phys. Educ.*
13, 351–352 (1978).
¹²L. Durand, "Stability and oscillations of a soap film: An analytic treat-
ment," *Am. J. Phys.* **49**, 334–343 (1981).
¹³M. A. Earle, R. D. Gillette, and D. C. Dyson, "Stability of interfaces of
revolution and constant surface tension—The case of the catenoid,"
Chem. Eng. J. **1**, 97–109 (1970).

Analogy between general relativity and electromagnetism for slowly moving particles in weak gravitational fields

Edward G. Harris

Department of Physics and Astronomy, University of Tennessee, Knoxville, Tennessee 37996-1200

(Received 30 March 1990; accepted for publication 8 August 1990)

Starting from the equations of general relativity, equations similar to those of electromagnetic theory are derived. It is assumed that the particles are slowly moving ($v \ll c$), and the gravitational field is sufficiently weak that nonlinear terms in Einstein's field equations can be neglected. For static fields, the analogy to electrostatics and magnetostatics is very close. Results are compared with those of a previous derivation by Braginsky, Caves, and Thorne [*Phys. Rev. D* **15**, 2047–2068 (1977)]. These results lead to very simple derivations of the Lense–Thirring precession [*Phys. Z.* **19**, 156–163 (1918)] and the spin-curvature force of Papapetrou [*Proc. R. Soc. London Ser. A* **209**, 248–258 (1951)] and Pirani [*Acta Phys. Pol.* **15**, 389–405 (1956)].

I. INTRODUCTION

Braginsky *et al.*¹ have derived equations similar to Maxwell's equations that describe a weak gravitational field. This has the advantage that many of the known results of electromagnetic theory may be applied to the gravitational field with only minor modifications. These equations deserve to be better known. The starting point for the derivation was the "parametrized post-Newtonian (PPN) formalism." We think a derivation that starts from the equations of general relativity and arrives rather quickly at a result is of interest. This is given below.

A particle of mass m and charge e moving in a gravitational and an electromagnetic field has the equations of motion

$$m \left[\frac{d^2 x^\mu}{d\tau^2} + \Gamma_{\alpha\beta}^\mu \left(\frac{dx^\alpha}{d\tau} \right) \left(\frac{dx^\beta}{d\tau} \right) \right] = \left(\frac{e}{c} \right) F_{\nu}^\mu \left(\frac{dx^\nu}{d\tau} \right), \quad (1a)$$

where

$$\Gamma_{\alpha\beta}^\mu = \frac{1}{2} g^{\mu\sigma} (\partial_\alpha g_{\sigma\beta} + \partial_\beta g_{\sigma\alpha} - \partial_\sigma g_{\alpha\beta}) \quad (1b)$$

are the components of the connection (Christoffel symbols) and

$$F^{\mu\nu} = \begin{vmatrix} 0 & -E_x & -E_y & -E_z \\ +E_x & 0 & +B_z & -B_y \\ +E_y & -B_z & 0 & +B_x \\ +E_z & +B_y & -B_x & 0 \end{vmatrix} \quad (1c)$$

is the electromagnetic field tensor. The coordinates are $x^\mu = (ct, x, y, z)$ and τ is the proper time. Greek indices take on

the values 0,1,2,3, and Latin indices take on the values 1,2,3. We write the metric tensor as $g_{\mu\nu} = \eta_{\mu\nu} + h_{\mu\nu}$ where $\eta_{\mu\nu}$ is the Lorentz metric whose only nonvanishing components are $\eta_{00} = -\eta_{11} = -\eta_{22} = -\eta_{33} = +1$. We assume the gravitational field is sufficiently weak so that $|h_{\mu\nu}| \ll 1$, and we raise and lower indices with $\eta^{\mu\nu}$ and $\eta_{\mu\nu}$. In a coordinate system in which the metric tensor is the Lorentz metric $\eta_{\mu\nu}$, the four-velocity is

$$\frac{dx^\mu}{d\tau} = \gamma(c, \mathbf{v}), \quad (1d)$$

where

$$\gamma = (1 - v^2/c^2)^{-1/2}.$$

If the particle is moving very slowly so that $v \ll c$, then it is a good approximation to write

$$\Gamma_{\alpha\beta}^\mu \left(\frac{dx^\alpha}{d\tau} \right) \left(\frac{dx^\beta}{d\tau} \right) \approx c^2 \Gamma_{00}^\mu + 2c \Gamma_{0j}^\mu v^j. \quad (2)$$

We write Eq. (1b) as $\Gamma_{\alpha\beta}^\mu = g^{\mu\sigma} \Gamma_{\sigma\alpha\beta}$ and find

$$\Gamma_{\sigma 0\beta} = \frac{1}{2} (\partial_\beta h_{0\sigma} + \partial_0 h_{\sigma\beta} - \partial_\sigma h_{0\beta}). \quad (3)$$

We see that for static fields, the term $\partial_0 h_{\beta\sigma} = 0$ and $\Gamma_{\sigma 0\beta} = -\Gamma_{\beta 0\sigma}$. This suggests that we divide $\Gamma_{\sigma 0\beta}$ into its antisymmetric and symmetric parts and write

$$\Gamma_{\sigma 0\beta} = -f_{\sigma\beta} + \partial_0 h_{\sigma\beta}/2, \quad (4a)$$

where

$$f_{\sigma\beta} = (\partial_\sigma h_{0\beta} - \partial_\beta h_{0\sigma})/2 = -f_{\beta\sigma}. \quad (4b)$$